Metallophysics and Advanced Technologies
Металофіз. новітні технол.
Metallofiz. Noveishie Tekhnol.
2022, vol. 44, No. 12, pp. 1629–1642
https://doi.org/10.15407/mfint.44.12.1629
Reprints available directly from the publisher

PACS numbers: 61.44.Br, 62.20.Qp, 68.35.Ct, 68.35.Np, 81.15.Rs, 81.40.Pq, 81.65.Kn

Microstructure and Tribological Properties of AlCuFeSc Coatings: Effects of Surface Roughness and Quasi-Crystalline *i*-Phase Content

Zhang Li, Changliang Wang, Chonggao Zhu, Haoliang Tian, Kostyantyn E. Grinkevych*, Mykola O. Iefimov*, Ivan V. Tkachenko*, and Sergey V. Buchakov*

Aviation Key Laboratory of Science and Technology on Advanced Corrosion and Protection for Aviation Material Beijing, Beijing Institute of Aeronautical Materials, 100095 Beijing, China
**I. M. Frantsevych Institute for Problems in Materials Science, N.A.S. of Ukraine, 3 Academician Krzhyzhanovsky Str., UA-03142 Kyiv, Ukraine*

High-velocity air–fuel (HVAF) spraying and detonation spraying (DS) methods are used to produce the Al–Cu–Fe–Sc coatings from a water-atomized powder on a low-carbon steel (Q235/SS330) substrate. X-ray diffraction phase analysis shows that the protective AlCuFeSc coatings produced by these methods contain different volume fractions of quasi-crystalline (QC) *i*-phase. Wear and friction behaviour of the produced AlCuFeSc coatings is studied in the dry and wet conditions depending on the loading type (quasi-static or dynamic) for various counter-bodies (Si_3N_4, WC–Co hard alloy, or 52100 bearing steel). The effects of the coating-surface roughness and the QC *i*-phase content are also analysed.

Key words: Al–Cu–Fe based quasi-crystal, protective coating, high-velocity air–fuel spraying, wear, friction.

Методи високошвидкісного повітряно-паливного напорошення (HVAF) і детонаційного напорошення (DS) використано для одержання покриттів Al–Cu–Fe–Sc з розпорошеного водою порошку на підкладинці з маловуг-

Corresponding author: Mykola O. Iefimov
E-mail: n.iefimov@ukr.net

Citation: Zhang Li, Changliang Wang, Chonggao Zhu, Haoliang Tian, Kostyantyn E. Grinkevych, Mykola O. Iefimov, Ivan V. Tkachenko, and Sergey V. Buchakov, Microstructure and Tribological Properties of AlCuFeSc Coatings: Effects of Surface Roughness and Quasi-Crystalline *i*-Phase Content, *Metallofiz. Noveishie Tekhnol.*, **44**, No. 12: 1629–1642 (2022). DOI: 10.15407/mfint.44.12.1629

лецевої криці (Q235/SS330). Рентґенівська фазова аналіза показує, що захисні покриття AlCuFeSc, одержані цими методами, містять різні об'ємні частки квазикристалічної (КК) *i*-фази. Поведінка одержаних покриттів AlCuFeSc за умов зношування та тертя вивчається в сухих і вологих умовах залежно від типу навантаження (квазистатичного або динамічного) для різних контртіл (Si_3N_4, твердий стоп WC–Co або підшипникова криця ШХ15). Також аналізується вплив шерсткости поверхні покриття та вміст КК *i*-фази.

Ключові слова: квазикристал на основі Al–Cu–Fe, захисне покриття, високошвидкісне повітряно-паливне напорошування, детонаційне напорошування, зношування, тертя.

(Received September 23, 2022)

1. INTRODUCTION

Highly wear-resistant alloys are important in many constructions engineering. Low-carbon steels are seemingly the most widely used materials in the machine building and construction industries, due to their low cost and satisfactory strength. However, the main issue to solve for the low/middle-carbon steels is the improvement of their corrosion, wear and fatigue resistance that are directly related to the surface conditions [1–3]. Therefore, additional surface protection is often essential and is usually provided by various types of coatings [3–5]. Good integrity and adhesion of the formed coating can save the underneath near-surface layers from corrosion and wear damage, and thus it may facilitate the prolonged fatigue life and overall component's feasibility.

The superior hardness and stiffness characteristics of quasi-crystals of the Al–Cu–Fe system facilitate low-friction, wear-resistant behaviour [6–9]. Therefore, the Al–Cu–Fe quasi-crystalline coating can be effective for protection of steel products. The QC AlCuFe coatings deposited by thermal or plasma spraying [10–12], by magnetron sputtering [13] electron beam (EB) PVD technique [14, 15] were also shown to possess a superior hardness and wear resistance that is comparable or even higher than that of the natural composites containing QC particles dispersed in the beta-phase matrix with b.c.c. lattice [16], multiphase alloys with QC strengthening [17], or artificial Al-based composite layers containing QC particles [18–21].

Complex solidification behaviour of the Al–Cu–Fe system may hinder the synthesis of macroscopic, single-phase quasi-crystals. Therefore, high-velocity air–fuel (HVAF) spraying technique that is known to allow controlling the temperature applied during the deposition process can be promising in the production of the coatings with controllable volume fraction of the QC phase, microstructure, and wear/friction properties of the produced coating. Moreover, it was re-

cently shown that the improvement of the stability and properties of the quasi-crystalline phase in the AlCuFe system can be achieved by additional alloying with scandium [22, 23].

The purpose of this work was to characterize and compare the wear and friction behaviour of the quasi-crystalline Al63Cu25Fe12Sc0.22 coatings on low-carbon steel produced by high-velocity air–fuel (HVAF) and detonation spraying (DS) techniques. Particular attention is given to the effects of the surface roughness, volume fraction of QC *i*-phase, test mode (quasi-static or dynamic load; dry or wet wear), and counter-body material (Si_3N_4, WC–Co hard alloy, or 52100 (GCr15) bearing steel) at the wear tests.

2. EXPERIMENTAL DETAILS

A high-velocity air–fuel (HVAF) spraying method was used to deposit an Al–Cu–Fe–Sc coatings on a low-carbon steel (St3/SS330/Q235) substrate. Prior the HVAF spraying process, the substrate was sand-blasted by quartz sand (particle size of $\cong 1$ mm) to form a clean and rough enough surface and provide better adhesion in the 'coating-substrate' system. An excess pressure of 1 MPa, stream velocity of $\cong 500$ m/s, oxidant excess factor $\alpha \approx 1.3$, and working temperature of $\cong 650$°C were sustained to be constant during the HVAF spraying process. Additionally, several coatings were deposited by detonation spraying method (DS) described elsewhere [24, 25].

In both cases, the water-atomized Al–Cu–Fe–Sc quasi-crystalline powder with particle size ranged 40–80 μm was used to produce the coatings. The chemical composition of the used powder was the following (in at.%): Al–61.75; Cu–25.56; Fe–12.44; Sc–0.25. The water-atomization method developed in IPMs N.A.S.U. [26–28] was shown to be effective for the production of the fully QC and QC containing powders of various systems (AlCuFe, AlFeTiCr) [24]. In this study, the melt prepared from A5 aluminium (99.95%), cathode copper (99.99%), Armco iron (99.92%), and industrial master alloy Al–2.46% Sc was atomized under the ARSAL 2120 flux by a high-pressure water at the cooling rate of 10^6 K/s.

The stripe-shaped samples of 2 mm thick were coated. The thickness of the HVAF and DS coatings was 225 ± 25 μm, respectively.

X-ray diffraction analysis using a DART-UM1 diffractometer in CuK_α irradiation was used to determine the phase composition of the water-atomized powders and produced coatings. The amount of the icosahedral QC phase was assessed based on the known correlation of the phase structure with the intensity of x-ray maxima from the quasi-crystalline and b.c.c. β-phases (a calibration curve was proposed in [11]). Scanning electron microscopy (SEM) using a Superbrobe-733 microscope was also used to monitor the structure of the resulting coat-

ings. Optical microscopy (Neophot-32 and the secant method) and ImagePro software were employed for the image analysis and the residual porosity estimation.

Wear losses and friction characteristics were examined using a computer assisted tribological complex (CATC) developed and located in IPMs (Kyiv, Ukraine) [18, 19, 27]. Sliding wear tests were carried out both in dry and wet (inactive liquid paraffin) conditions. The wear tests consisted in a reciprocating sliding movement of spherical indenters (Si_3N_4, WC–Co, and 52100 (GCr15) bearing steel) along a track of 4 mm long. The tests lasted for 20 min, and the sliding velocity was of 0.0147 m/s. Five duplicate runs were conducted for each material studied, and then statistically averaged. The variable of the test method was not exceeded 4%. Wear magnitudes for quasi-static (W_{st}) and dynamic (W_d) modes were characterized with the depth of wear tracks measured using P-201 profilograph-profilometer. The latter was also used to assess the surface roughness of the produced coatings. The friction force (F) was estimated *via* measured displacement of an elastic circular element rigidly connected to the tested specimen by induction transducer. Coefficient of friction (CoF) was also estimated in all cases. The worn surfaces were also examined using SEM (the Superbrobe-733 microscope). The CATC allowed conducting tests of two types [18, 19, 27]: (i) usual quasi-static wear test performed at quasi-static load (20 N) applied in a normal direction to the tested surface, and (ii) so-called dynamic wear test, which consisted in applying both the quasi-static and alternating components of the load. A frequency and duration of the latter were $5 \cdot 10^{-2}$ and 25 Hz, respectively. Amplitude of the alternating component of load was approx. 25% regarding to that of quasi-static one.

3. RESULTS AND DISCUSSION

3.1. Coating Microstructure and Phase Composition

Despite the same content of the QC phase (75%) in the water-atomized powder used for the coating productions, the phase compositions of the AlCuFeSc coatings produced by HVAF and DS methods were revealed to be different—these coatings respectively contain 75% and 20% of quasi-crystalline icosahedral ψ-phase (*i*-phase) and residual b.c.c. β-phase.

Figure 1 shows x-ray diffraction patterns for the initial water-atomized AlCuFeSc powder and deposited coatings produced by HVAF and DS methods. The observed XRD data confirm that the used HVAF regime provides the same content of the *i*-phase (Fig. 1, spectrum 1) as that in the initial powder (Fig. 1, spectrum 0), while the DS produced coating contain only 20% of the *i*-phase (Fig. 1, spectrum 2). This dif-

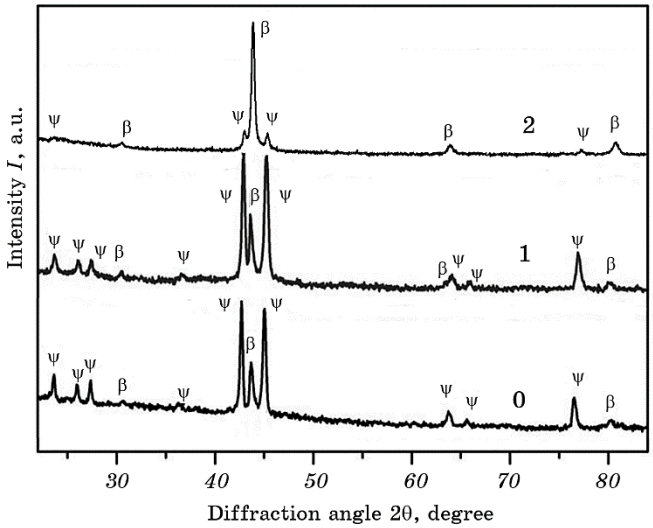

Fig. 1. X-ray patterns of the water-atomized AlCuFeSc powder (75% QC) (0) and AlCuFeSc coating deposited by HVAF (75% QC) (1) and DS (20% QC) (2) methods on a substrate made of low-carbon steel.

ference is seemingly related to the regimes (mainly temperature) used at the various deposition procedures.

SEM image shows the cross-section of the AlCuFeSc coating produced using HVAF spraying on the low-carbon steel substrate (Fig. 2). The observed coating comprises of quasi-crystalline icosahedral *i*-phase and residual b.c.c. β-phase, and the latter is visible as the lighter-grey areas since it contains higher content of copper. Some blackish interlayers are seemingly corresponded to residual porosity that was

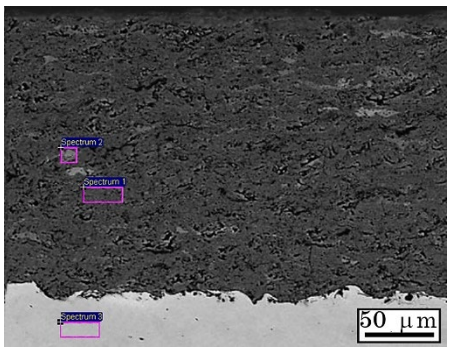

	Element content, at.%		
Spectrum	1	2	3
Phase	ψ	β	Substrate
Al	65.3	55.3	–
Cu	22.38	38.1	0.003
Fe	12.1	6.6	99.38
Sc	0.22	–	–
C	–	–	0.0005
Mn	–	–	0.003

Fig. 2. SEM image of the cross-section of the AlCuFeSc coating produced by HVAF spraying on the substrate made of low-carbon steel and chemical compositions of the indicated areas.

assessed to be lower than ≅ 8% (7–8% according to the secant method and 7.89% assessed by the ImagePro software). Owing to small average pore size (0.5–2 μm), the mechanical properties of the coating seem can be negligibly affected by the residual porosity.

3.2. Wear and Friction Behaviour

3.2.1. Effect of the Coating Surface Roughness and Lubrication

To assess the effect of the surface roughness of the AlCuFeSc coatings on their wear and friction behaviour the sliding wear tests against Si_3N_4 counter-body were carried out. There were compared the outputs of the AlCuFeSc coatings of high surface roughness, *i.e.*, directly after deposition, and after mechanical polishing to minimize the surface roughness (*Rz* = 0.3). Both quasi-static and dynamic loads on the counter-body were used. Additionally, dry and wet (liquid paraffin) condi-

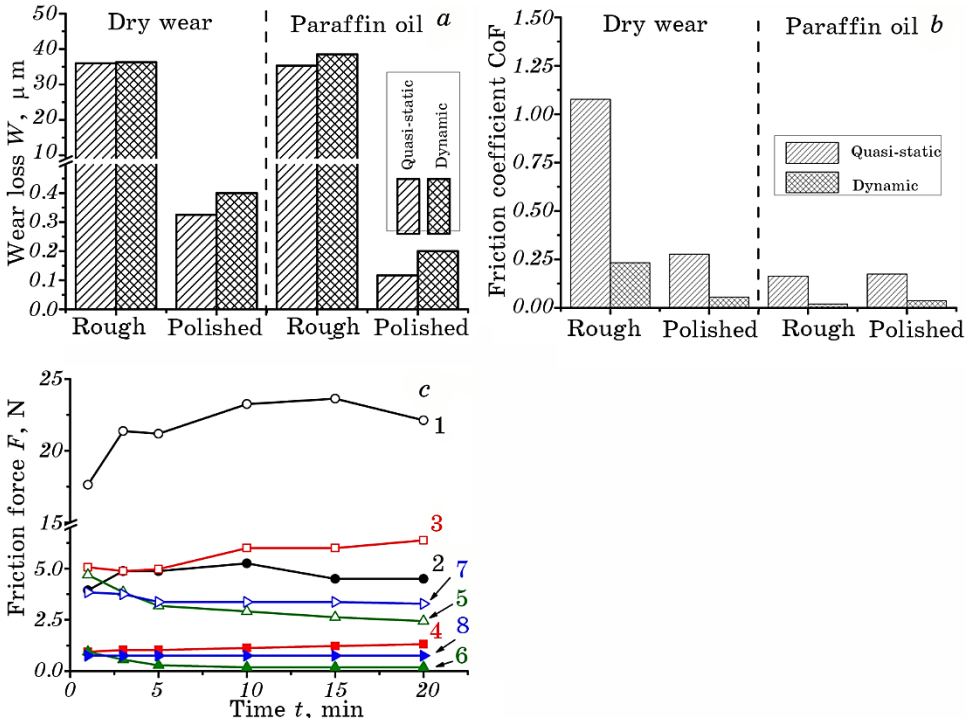

Fig. 3. Wear losses (*a*), friction coefficients CoF (*b*), the time dependences of friction force *F* (*c*) of the highly rough (1, 2, 5, 6) and polished (3, 4, 7, 8) DS-deposited AlCuFeSc coatings at a sliding wear against Si_3N_4 counter-body at quasi-static (1, 3, 5, 7) and dynamic (2, 4, 6, 8) loads and in dry (1–4) or wet (5–8) conditions.

tions were analysed. Figure 3 shows measured wear losses (*a*) and friction coefficients CoF (*b*) calculated based on the registered time dependences of the friction force *F* (*c*) of the DS-deposited AlCuFeSc coatings.

As seen, wear losses of the highly rough surface are much higher than those observed for the polished surfaces. Moreover, the wear environment (dry or wet wear conditions) does not change the wear loss values in this case static ($W_{st} \approx W_d$). Conversely, the mechanically polished surfaces of the DS-deposited AlCuFeSc coatings demonstrate lower wear losses in liquid paraffin than that registered in dry conditions. The deteriorative effect of the dynamic load is also revealed to higher in the case of the mechanically polished DS-deposited AlCuFeSc coatings (Fig. 3, *a*). Supposedly, for this highly rough coating surface, the wear debris early chipped/exfoliated from the surface layer may play a role of additional abrasive media in the contact area facilitating the increased wear loses. Subsequent mechanical polishing that minimizes the surface roughness prevents the polished coating surface from early fracture and the quantity of the chipped/exfoliated parti-

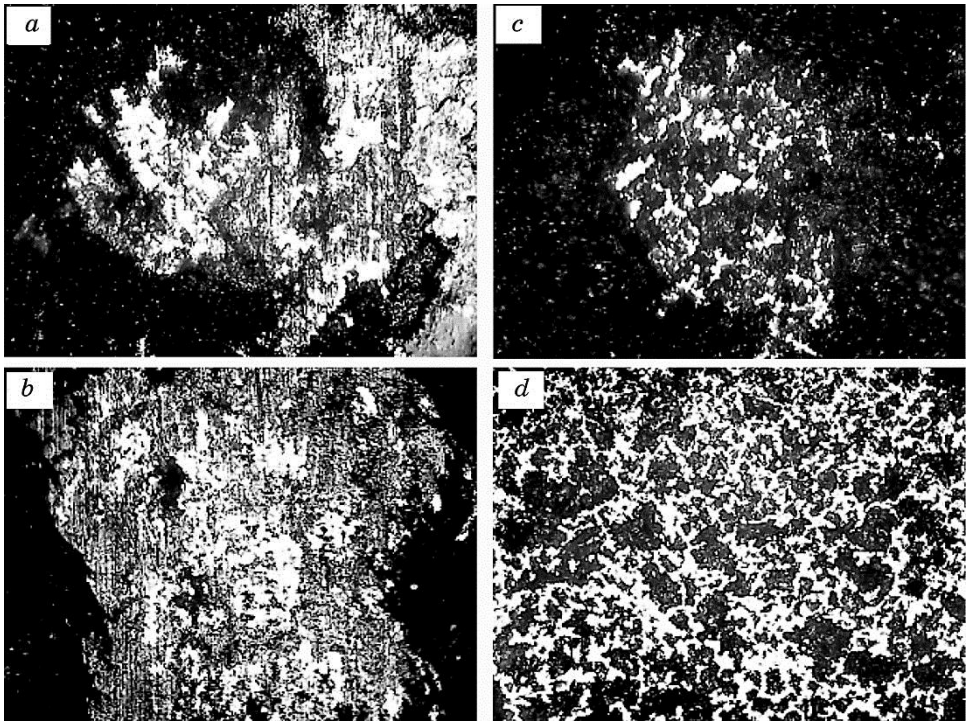

Fig. 4. Optical micrographs of the surface microreliefs in the wear tracks formed on the highly rough AlCuFeSc coating produced by DS at quasi-static (*a*, *c*) and dynamic (*b*, *d*) loads in dry (*a*, *b*) and wet (*c*, *d*) conditions.

cles becomes much lower. Thus, the abrasive part in the wear process become negligible and this polished coating demonstrates better wear resistance.

The afore-mentioned reasons are confirmed by optical micrographs of the surface microreliefs in the wear tracks formed on the highly rough AlCuFeSc coating produced by DS method (Fig. 4). Both the quasi-static and dynamic loads result in similar wear surfaces irrespective to the test environment used (dry or wet conditions). The microreliefs of the observed wear tracks formed in various wear test conditions have distinct differences. First, dynamically loaded indenter leads to higher wear losses. Second, the liquid paraffin environment provides the absence of the wear burrs, which are normally observed in the case of micro-abrasion and microwelding (for high CoF).

3.2.2. Effect of Volume Fraction of QC Phase

This section compares the wear and friction characteristics of the HVAF sprayed and DS deposited AlCuFeSc coatings that contained different volume fractions of the QC *i*-phase. These characteristics were evaluated at the wear tests against the counter-body made of the Si_3N_4 ceramics at quasi-static and dynamic loads in wet conditions (inactive liquid paraffin oil).

It should be pointed out that due to the differences in the production technologies the studied coatings had slightly different thickness. Additionally, for the DS-deposited coatings the thickness of the used steel substrate was five times lower than that used for fabrication of the HVAF sprayed coating. In some extent, these features may affect the registered data owing to the differences in the substrate damping property, and they should be taken into account at further analysis of them. Figure 5 shows measured wear losses (*a*) and friction coefficients CoF (*b*) calculated based on the registered time dependences of the friction force *F* (*c*) of the HVAF sprayed and DS-deposited AlCuFeSc coatings.

As seen, wear losses of the HVAF sprayed AlCuFeSc coatings with higher volume fraction of the QC *i*-phase are larger than those registered for the DS-deposited coatings at the quasi-static and dynamic loads (Fig. 5, *a*). However, the wear losses registered at the static tests (W_{st}) always lower than those registered at dynamic loads (W_d). Supposedly, the QC *i*-phase possessing very low fracture toughness ($K_{1C} = 1.64$ MPa·m$^{0.5}$ [28, 29]) might undergo easier fracture than the b.c.c. beta phase. It thus may facilitate quicker chipping/delaminating the wear debris that further might play a role of additional abrasive medium. It is of importance that the friction coefficients (CoF) are almost the same for both studied coatings and both loading conditions (Fig. 5, *b*). More precise analysis of the time dependencies of the fraction forces for the studied AlCuFeSc coatings with different volume fractions of the QC *i*-

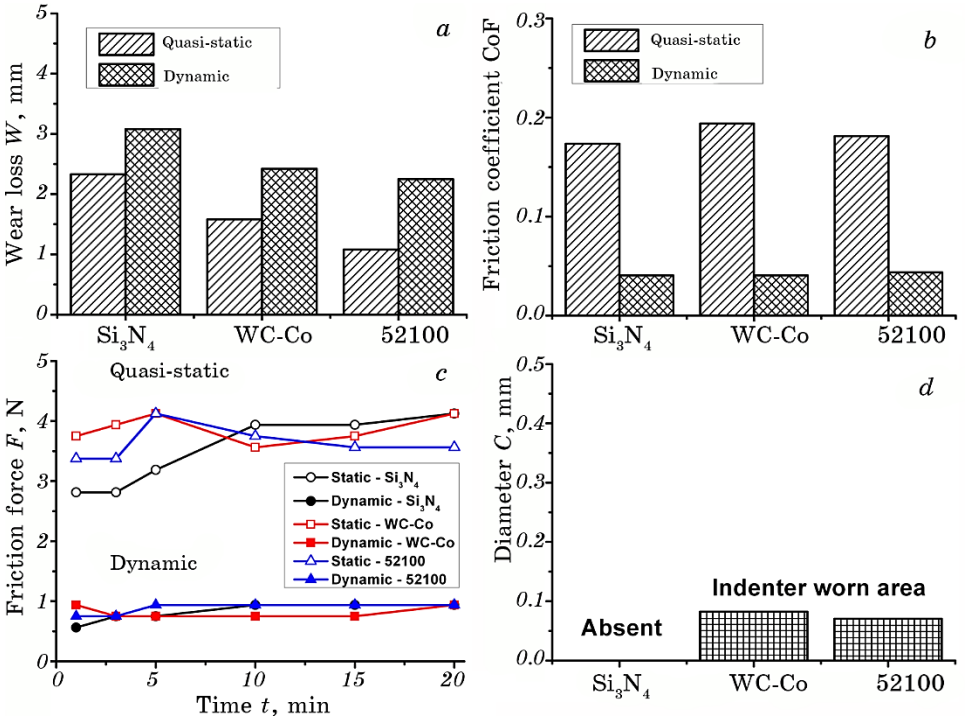

Fig. 5. Wear losses (*a*), friction coefficient CoF (*b*), the time dependence of friction force *F* (*c*) of the HVAF and DS-deposited AlCuFeSc coatings on the low-carbon steel substrate at sliding wear against Si_3N_4 counter-body in inactive liquid paraffin oil.

phase shows that the fraction forces registered for the HVAF sprayed AlCuFeSc coatings (75% content of QC phase) at both used loading types (static and dynamic ones) are lower on the first stages of the wear process, but they became higher than those registered for the DS-deposited AlCuFeSc coatings (20% content of QC phase) after the wear test duration of 5–7 minutes (Fig. 5, *c*).

3.2.3. Effect of the Counter-Body

To examine possible practical use of the AlCuFeSc coatings and to assess the reproducibility of the test results the wear and friction characteristics were evaluated at the wear tests against various counter-bodies. The Si_3N_4 ceramics, a WC–Co hard alloy frequently used for the hard-facing instruments, and 52100 (GCr15) bearing steel are widely used materials for bearings. Wear losses and friction characteristics examined using a reciprocating sliding movement of the aforementioned spherical indenters are shown in Fig. 6.

As seen, maximal wear loses were observed after wear test against the counter-body made of Si_3N_4, a minimal damage in the coating was observed for the counter-body made of bearing steel (52100/GCr15) (Fig. 6, *a*). This situation can be explained by the different hardness of the used counter-bodies. At the same time, the friction force and CoF were minimal at the tests against the Si_3N_4 ceramics although the friction forces and CoF values were very similar for all the used counter-bodies (Fig. 6, *b*, *c*, Table 1). Normally, the friction forces measured at the dynamic loads were much lower than those registered for the static ones were (Fig. 6, *c*). Additionally, no worn marks were observed for this counter-body after wear tests. On the contrary, both the WC–Co hard alloy and 52100 (GCr15) bearing steel worn during the tests together with the studied AlCuFeSc coatings, and the worn areas were measured to be about 0.1 mm (Fig. 6, *d*). Minimal wear loses of AlCuFeSc coatings were observed after wear tests against the counter-body made of S bearing steel [30, 31].

Generally, the studied AlCuFeSc coatings demonstrate excellent

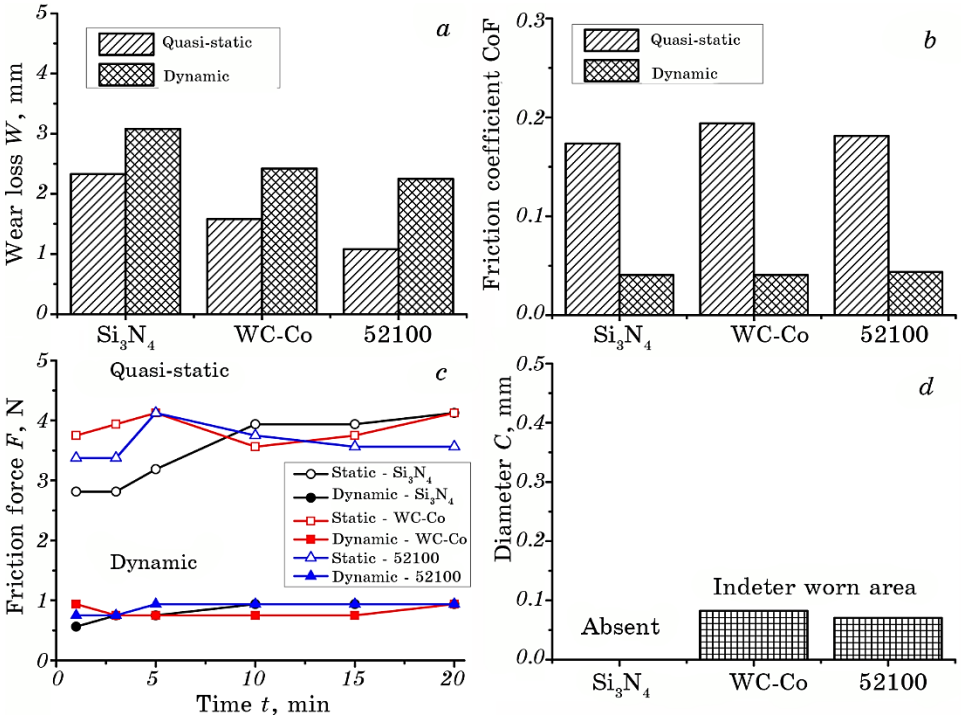

Fig. 6. Wear losses (*a*), friction coefficient CoF (*b*), the time dependence of friction force *F* (*c*) of the HVAF sprayed AlCuFeSc coating on the low-carbon steel substrate at sliding wear against various counter-bodies, and the indenter worn area diameters C on the indenter surface (*d*).

TABLE 1. Friction coefficient CoF values of the AlCuFeSc coating produced using HVAF spraying on the low-carbon steel substrate.

Counter-body	Friction coefficient CoF	
	Quasi-static load	Dynamic load
Si_3N_4 ceramics	0.17344	0.04063
WC–Co hard alloy	0.19375	0.04063
52100 (GCr15) bearing steel	0.18125	0.04375

wear resistance and very low friction coefficient values against all the used counter-bodies. This conclusion is confirmed by the optical and SEM images of the worn surfaces shown in Fig. 7.

Wear tracks can hardly be found in the SM images, and thus they are indicated by arrows. It is of interest that the coating surfaces remain wear resistant despite the apparent scaly surface views.

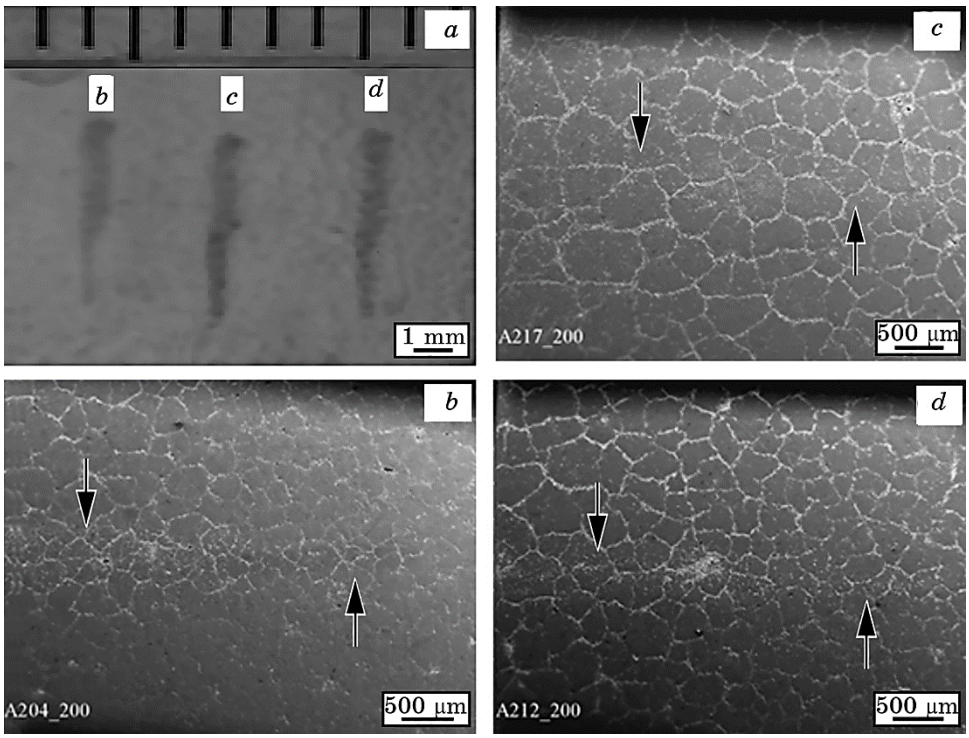

Fig. 7. Optical image of the wear tracks (*a*) and SEM images of wear surfaces (*b*–*d*) formed on the AlCuFeSc coating produced by HVAF spraying on the substrate made of low-carbon steel reciprocating sliding movement of by spherical indenters made of Si_3N_4 ceramics (*b*), WC–Co (*c*), and GCr15 bearing steel (*d*). Arrows indicate the wear tracks.

4. CONCLUDING REMARKS

As shown, method of high-velocity air–fuel (HVAF) spraying and detonation spraying (DS) techniques can be efficient in the formation of protective AlCuFeSc coatings on a low-carbon steel (Q235/SS330) from the water-atomized quasi-crystalline powders. X-ray analysis and SEM observations show that the HVAF sprayed and DS deposited AlCuFeSc coatings contain different volume fractions of AlCuFeSc quasi-crystalline icosahedral ψ-phase, 75% and 20%, respectively.

Generally, all the studied AlCuFeSc quasi-crystalline phase containing coatings showed excellent wear resistance and very low coefficient of friction CoF, especially at dynamic loading and wet conditions. Therefore, these coatings can be used for anti-wear protection of the products made of low-carbon steel (Q235/SS330).

As shown, the higher the surface roughness of the tested coating the higher the wear losses are irrespectively to the test conditions (static/dynamic loading and dry/wet wear testing). A difference on an order of magnitude is registered between the highly rough and mechanically polished ($Rz = 0.3$) coating surfaces. The highest friction coefficient is observed for rough surfaces tested in dry conditions, while these rough surfaces tested in wet conditions and the polished surface examined in both dry and wet test conditions demonstrated four times lower CoF values ($\cong 0.2–0.25$) at quasi-static loads and about ten times lower at dynamic loads (0.05–0.1).

As shown, during the wear tests against the Si_3N_4 ceramic counterbody in inactive liquid paraffin oil, the higher the QC *i*-phase content the larger the wear losses. At the same time, the friction force values are the same regardless the QC volume fractions—they are as small as 0.18 and 0.04 for the HVAF (75% of QC *i*-phase) and DS deposited (20% of QC *i*-phase) AlCuFeSc coatings, respectively.

As shown, maximal, middle and minimal wear loses of the HVAF sprayed AlCuFeSc coatings were observed after wear test against the counter-bodies made of Si_3N_4 ceramics, WC–Co hard alloy and 52100/GCr15 bearing steel, accordingly. The magnitudes of the friction coefficient CoF evaluated based on the registered time dependencies of the friction force were almost the same for various used counter-bodies, but they were extremely lower for the dynamic loading conditions ($\cong 0.035$) as compared to those registered for the quasi-static loading conditions ($\cong 0.17–0.19$).

ACKNOWLEDGEMENTS

Sponsorships by the National Natural Scientific Foundation of China (52075508), National Science and Technology Major Project (2017-VII-0012-0109), Beijing Nova Program (Z191100001119040) are

acknowledged. The authors also thank Dr. V. Kisyl and Dr. Yu. Yevdokimenko for obtaining HVOF coatings.

REFERENCES

1. M. P. Nascimento, R. C. Souza, I. M. Miguel, W. L. Pigatin, and H. J. C. Voorwald, *Surf. Coat. Technol.*, **138**: 113 (2001).
2. D. A. Lesyk, S. Martinez, B. N. Mordyuk, V. V. Dzhemelinskyi, A. Lamikiz, G. I. Prokopenko, M. O. Iefimov, and K. E. Grinkevych, *Wear*, **462–463**: 203494 (2020).
3. B. N. Mordyuk, G. I. Prokopenko, K. E. Grinkevych, N. A. Piskun, and T. V. Popova, *Surf. Coat. Technol.*, **309**: 969 (2017).
4. G. Contreras, C. Fajardo, J. A. Berríos, A. Pertuz, J. Chitty, H. Hintermann, and E. S. Puchi, *Thin Solid Films*, **355–356**: 480 (1999).
5. M. J. Ortiz-Mancilla, C. Marico-Berroterán, J. A. Berríos-Ortiz, G. Mesmacque, and E. S. Puchi-Cabrera, *Surf. Eng.*, **20**: 345 (2004).
6. J. M. Dubois, S. S. Kang, and J. Von Stebut, *J. Mater. Sci. Let.*, **10**: 537 (1991).
7. S. S. Kang, J. M. Dubois, and J. Von Stebut, *J. Mater Res.*, **8**: 2471 (1993).
8. D. J. Sordelet, M. F. Besser, and J. L. Logsdon, *Mater. Sci. Eng. A*, **255**: 54 (1998).
9. J.-M. Dubois, *Mater. Sci. Eng. A*, **294–296**: 4 (2000).
10. D. J.Sordelet, M. J.Kramer, and O. Unal, *J. Thermal Spray Technol.*, **4**: 235 (1995).
11. D. J. Sordelet, M. F. Besser, and L. E. Anderson, *J. Thermal Spray Technol.*, **5**: 161 (1996).
12. E. Fleury, S. M. Lee, W. T. Kim, and D. H. Kim, *J. Non-Cryst. Solids*, **278**: 194 (2000).
13. M. Cekada, P. Panjan, D. Juric, J. Dolinsek, and A. Zalar, *Thin Solid Films*, **459**: 267 (2004).
14. M. O. Iefimov, D. V. Lotsko, Yu. V. Milman, A. L. Borisova, S. I. Chugunova, Ye. A. Astakhov, and O. D. Neikov, *High Temp. Mater. Proc.*, **25**: 31 (2006).
15. Yu. V. Milman, D. V. Lotsko, S. N. Dub, A. I. Ustinov, S. S. Polishchuk, and S. V. Ulshin, *Surf. Coat. Technol.*, **201**: 5937 (2007).
16. K. Q. Lee, Y. Chen, W. Dai, D. Naugle, and H. Liang, *Mater. Des.*, **193**: 108735 (2020).
17. K. Q. Lee, J. L. Hsu, D. Naugle, and H. Liang, *Mater. Des.*, **108**: 440 (2016).
18. B. N. Mordyuk, M. O. Iefimov, K. E. Grinkevych, A. V. Sameljuk, and M. I. Danylenko, *Surf. Coat. Technol.*, **205**: 5278 (2011).
19. B. N. Mordyuk, G. I. Prokopenko, Y. V. Milman, M. O. Iefimov, K. E. Grinkevych, A. V. Sameljuk, and I. V. Tkachenko, *Wear*, **319**: 84 (2014).
20. N. Kang, Y. Q. Fu, Pierre Coddet, B. Guelorget, H. Liao, and C. Coddet, *Mater. Des.*, **132**: 105 (2017).
21. M. Galano, F. Audebert, A. Garcia Escorial, I. C. Stone, and B. Cantor, *Acta Mater.*, **57**: 5120 (2009).
22. Yu. V. Milman, D. V. Lotsko, and O. I. Sirko, *Mater. Sci. Forum.*, **331–337**: 1107 (2000).
23. Yu. V. Milman, *High Temp. Mater. Proc.*, **25**, Nos. 1–2: 1 (2006).
24. O. D. Neikov, *Proc. of 2000 Powder Metallurgy World Congress* (Kyoto: Japan

Society of Powder Metallurgy: 2000), p. 464.
25. O. D. Neikov, S. S. Naboychenko, I. B. Murashova, and N. A. Iefimov, *Handbook of Non-Ferrous Metal Powders* (Ed. O. D. Neikov) (Amsterdam: Elsevier: 2019), p. 685.
26. H. L.Tian, M. Q. Guo. C. L. Wang. Z. H. Tang, and Y. J. Cui, *Surf. Eng.*, **34**, No. 10: 762 (2018).
27. H. L. Tian, C. L. Wang, M. Q. Guo, Y. J. Cui, J. G. Gao, and Z. H. Tang, *Friction*, **9**, No. 2: 315 (2021).
28. N. A. Iefimov, *Handbook of Non-Ferrous Metal Powders* (Ed. O. D. Neikov) (Amsterdam: Elsevier: 2019), p. 313.
29. Yu. V. Milman, K. Grinkevich, S. Chugunova, W. Lojkowski, M. Djahanbakhsh, and H. J. Fecht, *Wear*, **258**: 77 (2005).
30. U. Köster, W. Liu, H. Liebertz, and M. Michel, *J. Non-Cryst. Solids*, **153–154**: 446 (1993).
31. B. N. Mordyuk, Y. V. Milman, M. O. Iefimov, and K. E. Grinkevych, *J. Manuf. Technol. Research*, **9**, Iss. 3: 4 (2017).